Journal of Power Sources 196 (2011) 5659–5666

Contents lists available at ScienceDirect

Journal of Power Sources

journal homepage: www.elsevier.com/locate/jpowsour

Solid-state nuclear magnetic resonance studies of electrochemically discharged CF_x

J.H.S.R. DeSilva[a,b], Rafael Vazquez[a,b], Phillip E. Stallworth[a,b], Thomas B. Reddy[c], Joseph M. Lehnes[d], Rui Guo[d], Hong Gan[d], Barry C. Muffoletto[d], Steven G. Greenbaum[a,b,*]

[a] Department of Physics and Astronomy, Hunter College of CUNY, New York, NY 10065, USA
[b] Ph.D. Program in Physics, CUNY Graduate Center, New York, NY 10016, USA
[c] Department of Materials Science and Engineering, Rutgers University, New Brunswick, NJ 08854, USA
[d] Greatbatch, Incorporated, Clarence, NY 14031, USA

ARTICLE INFO

Article history:
Received 7 January 2011
Received in revised form 9 February 2011
Accepted 12 February 2011
Available online 21 February 2011

Keywords:
Lithium batteries
Carbon monofluoride
Solid state nuclear magnetic resonance

ABSTRACT

Electrochemical studies of three types of CF_x (F – fiber based, C – petroleum coke based, G – graphite based) have demonstrated different electrochemical performances in previous work, with fiber based CF_x delivering superior performance over those based on petroleum coke and graphite. ^{13}C and ^{19}F MAS (magic angle spinning) NMR techniques are employed to identify the atomic/molecular structural factors that might account for differences in electrochemical performance among the different types of CF_x. Small quantitative variations of covalent CF and LiF are noted as a function of discharge and sp^3 bonded carbons are detected in discharged F type of CF_x.

1. Introduction

The lithium/carbon monofluoride cathode system is known to have the highest theoretical energy density among solid cathode systems. Li/CF_x batteries [1] have remained attractive because of their very high energy density, long storage life, very good safety record, wide temperature range and very low self-discharge. However its use is restricted to specialized applications where superior performance is required such as aerospace, military and medical applications due to the relatively high cost of CF_x.

Typically x is approximately equal to one for commercial grade Li/CF_x battery material. The electrolyte typically consists of lithium tetrafluoroborate ($LiBF_4$) in gamma-butyrolactone or lithium hexafluoroasenate ($LiAsF_6$) in a mixture of propylene carbonate (PC) and dimethoxyethane (DME) [2]. The chemical reaction of the discharging process is summarized below.

$$n\mathrm{Li} \rightarrow n\mathrm{Li}^+ + ne^- (\text{anode reaction})$$

$$ne^- + (\mathrm{CF}_x)_n \rightarrow n\mathrm{C} + n\mathrm{F}^- (\text{cathode reaction})$$

$$n\mathrm{Li} + (\mathrm{CF}_x)_n \rightarrow n\mathrm{LiF} + n\mathrm{C} (\text{overall reaction})$$

The CF_x is converted into elemental carbon which is more conductive than CF_x thereby lowering the internal impedance, improving the voltage regulation and the efficiency. At the same time LiF is formed and precipitates out of the structure during the course of discharge.

Electrochemical studies have shown significant differences between each type of CF_x: prepared from carbon with a fiber morphology, hereafter referred to CF_x – F or F-type; prepared from petroleum coke, hereafter referred to as CF_x – C or C-type; and prepared from graphite, hereafter referred to as CF_x – G, or G-type. Although the fundamentals of the electrochemical discharging process are known, the structure of the CF_x cathode during the discharge and the mechanism of the defluorination process at the molecular level that might be responsible for the electrochemical differences are not known. This study is focused on NMR investigations of these three different types of CF_x materials to determine their structural/chemical differences, discharge mechanism and possible intermediate compound formation during discharge.

2. Experimental

CF_x materials (F, C and G types) were prepared by fluorination of fibrous, amorphous coke and standard graphite respectively at 300–600 °C provided by commercial sources. Unfortunately no further details were provided by the vendor. CF_x cathode mixes were prepared with raw CF_x, conductive carbon, and binder materials.

* Corresponding author at: Department of Physics and Astronomy, Hunter College of CUNY, New York, NY 10065, USA. Tel.: +1 212 772 4973; fax: +1 212 772 5390.
E-mail address: steve.greenbaum@hunter.cuny.edu (S.G. Greenbaum).

0378-7753/$ – see front matter © 2011 Elsevier B.V. All rights reserved.
doi:10.1016/j.jpowsour.2011.02.036

Table 1
DoD levels of Greatbatch discharged samples.

CF_x – F%	CF_x – C%	CF_x – G%
1.2	1.2	1.2
7.5	7.9	7.8
22.2	23.0	23.3
45.2	46.5	45.4
67.2	69.8	67.9
89.3	92.1	86.7
97.0	99.4	95.6

Li/CF_x experimental cells were constructed with the three types of CF_x and they were discharged to various depth of discharge (DoD) under a 6 month discharge rate at 37 °C.

^{13}C (spin 1/2) MAS NMR, is widely used, despite its relative paucity in naturally occurring carbon (approximately 1%). Because of low natural abundance and generally long spin–lattice relaxation time (T_1), spectrum acquisition on samples which have not been experimentally enriched in ^{13}C takes a long time. A Varian Inova 500 MHz spectrometer and Doty low C/F background probe were used to perform ^{13}C MAS NMR measurements. Samples were packed in 4 mm rotors and spun up to 12–14 kHz. Tetramethylsilane (TMS) was used as the external reference.

^{19}F (spin 1/2) MAS NMR, is relatively commonly measured, yields strong signals and has a wide chemical shift range. ^{19}F MAS NMR measurements were conducted with a 300 MHz Varian S Direct Digital Drive NMR spectrometer (the 300 MHz spectrometer was used because of the availability of higher spinning speeds) at spinning speeds from 32 kHz to 37 kHz in 1.6 mm rotors. A 90_x–180_y pulse echo sequence was used to minimize the probe background signal. An aqueous solution of lithium trifluoromethylsulfonate was used as an external reference for fluorine at −77.8 ppm relative to the common reference $CFCl_3$. All the spectral analysis and deconvolution are performed by MestReNova software.

2.1. Deconvolution calibrations

The accuracy of deconvolution techniques and associated software was tested with known physical mixtures of raw CF_x – G and LiF. Four different mixtures of LiF/CF_x – G (LiF by weight – 10%, 20%, 50%, 75%) were investigated.

2.2. Slow (Greatbatch) discharged cells

Li/CF_x cells were electrochemically discharged for 6 months. The cell discharge voltage profiles and cell internal resistance vs. the DoD were obtained. Cathode materials were extracted at different DoD levels (Table 1) and washed thoroughly with DME to remove residual electrolyte salt.

Powder X-ray diffraction (XRD) measurements of discharged CF_x samples were performed using a Shimadzu X-ray diffractometer XRD-6000, working with a CuKα radiation. SEM images were obtained by using a LEO 1455VPSE scanning electron microscope. ^{19}F and ^{13}C studies were conducted (1–3 months) after sample preparation. Apart from MAS NMR measurements, nine samples (three of each type) were picked among 21 samples to perform ^{7}Li and ^{19}F T_1 measurements with inversion recovery pulse sequence.

2.3. Fast (Hunter) discharged cells

A focus of this study was to detect and investigate any short-lived intermediate species during the discharge process. NMR measurements were done in a short period of time (1–2 h) after cell discharge to improve the probability of detecting any metastable compounds. Six Li/CF_x batteries (two of each type) were electrochemically discharged at the Hunter lab with an Arbin battery cycler with a particular discharge protocol described below.

Table 2
Battery discharge protocol at Hunter.

CF_x battery type	Discharged time (h)	Target % DoD
F/C/G	309.12	46
F/C/G	537.60	80

Cells were discharged at room temperature under 2.93 mA constant current according to Table 2. After the long discharge, cells were equilibrated at open circuit and discharged again for a short period of time (1 min) at higher rate (75 mA) just before cell disassembly and NMR experiments. One particular cell (type C) with an estimated DoD of 80% could not sustain the short discharge at 75 mA, due to the cell having exceeded the voltage limit set for the procedure. A possible reason for this is mentioned later. Therefore it was discharged for 3 min at 25 mA instead of 1 min at 75 mA to acquire the target DoD.

Each battery was dissembled inside the argon filled glove-box. The cathode was extracted carefully and half of it was left alone and labeled as un-washed while the other half was rinsed with DME three times for 15 min each (labeled as washed). ^{13}C and ^{19}F MAS NMR studies of un-washed samples were performed immediately after the disassembly. Washed samples were left inside of the glove box antechamber for several hours to dry completely before NMR studies.

3. Results and discussion

High speed MAS at 32–37 kHz greatly reduces the homonuclear dipolar coupling broadening of ^{19}F spectra, shown in Fig. 1 for the case of mixtures of CF_x and LiF. Sidebands were clearly identifiable and most of the features were easily distinguishable with no significant overlap. In discharged materials, four main features are prominent to different degrees depending on the sample that was studied. The most intense peak in all series at low discharge levels is around −184 to −187 ppm and was clearly larger for correspondingly lower level discharged samples, lower for higher level discharged samples, and assigned to covalent CF groups [3]. A semi-ionic CF peak is found around −170 ppm [2]. The broad peak around −113 to −116 ppm was assigned to CF_2 groups located at the edge of graphite layers [3,4]. A relatively sharp Teflon™ (present as a binder) peak occurs around −121 ppm. Upon discharging, the LiF

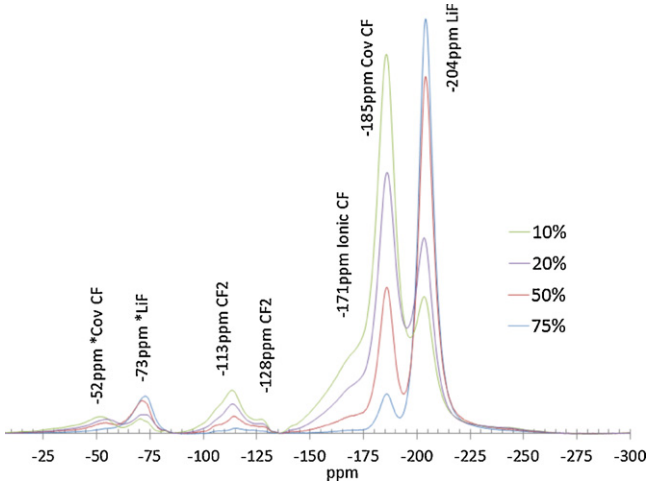

Fig. 1. ^{19}F MAS NMR of manually mixed LiF/CF_x mixtures. The percentages given above refer to the fraction of LiF in the mixture. Asterisks denote spinning sidebands.

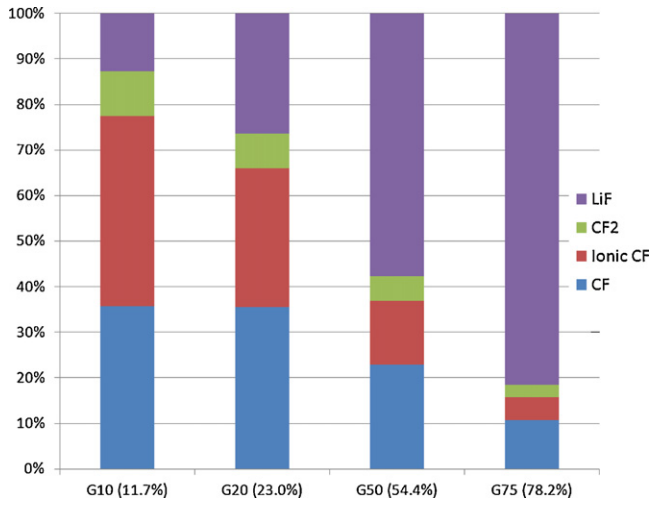

Fig. 2. ^{19}F MAS NMR deconvolution of manually mixed LiF/CF_x mixtures. Numbers are molar percentages which correspond to weight percentage values in Table 3.

resonance appears around −204 ppm [2]. Very slight changes of the positions of sidebands correspond to slight spinning speed variations. However this had a negligible effect on deconvolution and interpretation of the data.

3.1. Deconvolution calibrations

Right sidebands are not shown in the spectra (Fig. 1) for the sake of clarity but they have been included in the deconvolution shown in Fig. 2. LiF weight percentages were calculated from deconvolutions. Table 3 reveals that NMR measurements/deconvolution were very consistent with molar-weight-calculated values, although there is some uncertainty in deconvoluting the ionic and covalent CF features due to overlap (their ratios should not change in these spectroscopic standards).

3.2. Slow (Greatbatch) discharged batteries

CF_x experimental cells were discharged under a 6 month rate at 37 °C. The cell discharge voltage profiles are shown in Fig. 3. CF_x G cells show a more sloped discharge voltage profile than CF_x C and CF_x F cells. At beginning of life, CF_x G cells exhibit higher cell voltages than that of CF_x C and CF_x F cells. The CF_x G cell voltages gradually decrease and cross over at around 20% to 35% DoD resulting in lower cell voltages than that of CF_x C and CF_x F cells at later DoDs. The voltage profile of CF_x C cells is slightly higher than that of CF_x F cells throughout discharge. Both CF_x C and CF_x F cells exhibit a voltage plateau at around 2.8 V until ∼60% DoD and then gradually decrease. The discharge voltages from all three types of CF_x cells merge to 2.3 V at approximately 95% DoD.

Fig. 4 shows the relationship of the cell internal resistance (Rdc) vs. DoD. As expected, all cells exhibit decreased Rdc when they were discharged from BOL to ∼30% DoD due to the formation of carbon as one of the products. However, in the 2nd half of cell discharge, the cell Rdc starts to increase. For CF_x C, the cells have the lowest

Table 3
Comparison of weight percentage of LiF in known mixtures of CF_x – G and LiF with spectroscopic determination.

Percent from known mixture	Percent from NMR deconvolution
10.0	10.3
20.0	22.1
50.0	51.4
75.0	77.2

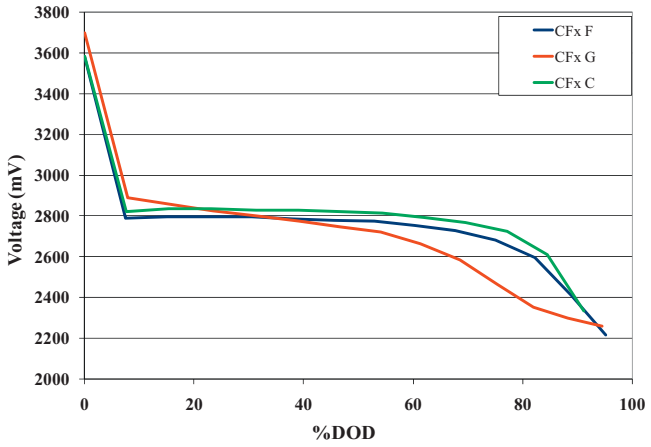

Fig. 3. Discharge voltage profiles of CF_x F, CF_x G, and CF_x C cells under 6 month discharge rate.

Rdc from BOL to ∼35% DoD. Beyond 35% DoD, CF_x C cells develop higher internal resistance relative to the cells from CF_x G and CF_x F. Beyond 80% DoD, CF_x C cells exhibit a significant Rdc increase, about 7 times that of the other two CF_x types. This could be related to the cell's response to the 75 mA pulse discharge described in the experimental section. Among the three types of CF_x, CF_x F cells exhibit the best stability with the least Rdc increase throughout discharge.

All three types of CF_x materials were electrochemically discharged to form carbon and LiF as the only detectable products as indicated by the XRD spectra shown in Fig. 5. The CF_x peaks at 13° and 42° are observed to deplete with increasing lithiation coincident with the increase in the prominence of the LiF peaks observed at 38°, 45°, 65° and 79°. A diffraction peak near 25°, which increases continuously with increasing lithiation, is assigned to graphite. The sharp LiF peaks indicate the crystalline nature of the LiF product. Further supporting evidence of the crystalline nature of the LiF is shown in the SEM images where cubic shaped crystals are observed in the lithiated samples, as shown in the case of CF_x – C in Fig. 6.

^{19}F NMR spectra for very slightly discharged materials (1.2% DoD) are shown in Fig. 7. The G type has the maximum covalent CF content and lower semi-ionic CF. The sum of both covalent CF and semi-ionic CF in the 1.2% discharged F, C and G samples is about 81%, 84% and 89% respectively of the total fluorine. The spectral intensity of the Teflon™ peak was excluded from the deconvolutions based

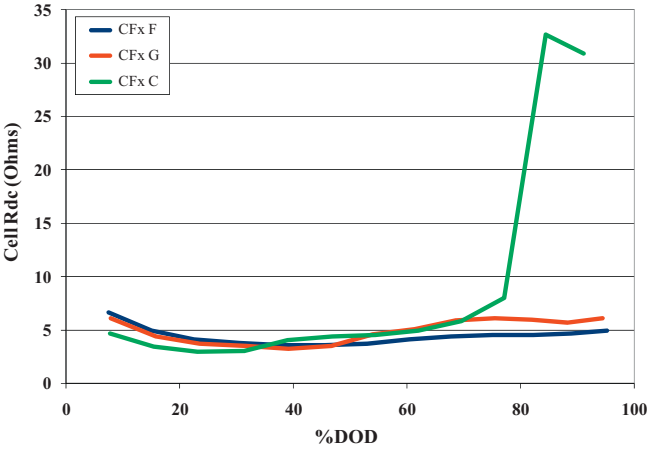

Fig. 4. CF_x type effect on cell internal Rdc change vs. %DoD.

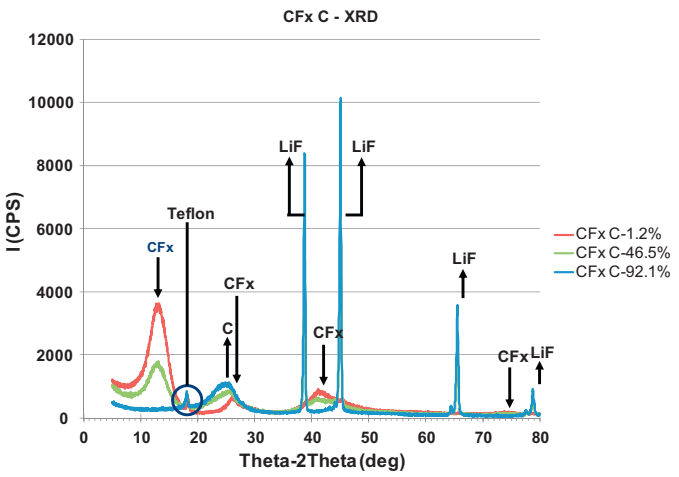

Fig. 5. X-ray diffractograms of CF_xC at three different DoD values.

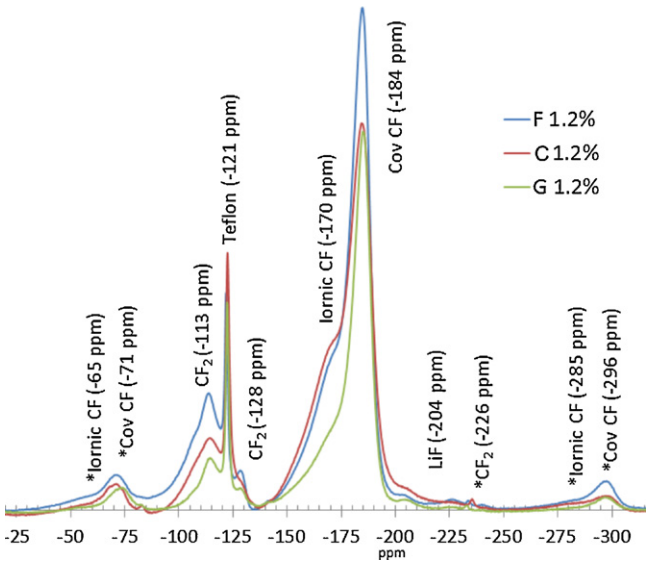

Fig. 7. ^{19}F MAS NMR spectra of Greatbatch discharged nearly starting materials (F, C, G). Asterisks denote spinning sidebands.

on the assumption that it is chemically inert throughout discharge. As expected CF and LiF peaks dominate the lower DoD levels and higher DoD levels, respectively, as shown in Fig. 8 for the F series. G series shows the highest covalent CF throughout the whole range of discharge followed by C and F as shown in the deconvolutions displayed in Fig. 9. A structural re-arrangement could be responsible for the small increase of covalent CF in first few DoD levels (around 7 to 8%), although this value is close to the deconvolution uncertainty of these two species as described earlier in the context of the manually mixed standards. The CF_2 content appears to decrease gradually upon discharging. In all three series, the semi-ionic CF is consumed faster than covalent CF in the electrochemically discharged cells, contrary to what was reported in chemically lithiated materials[2] (which is a comparatively very rapid process). Also no CF_3 groups around −50 to −70 ppm were noted as observed in previous results[2] for chemically lithiated CF_x.

^{13}C MAS NMR spectra were broader with lower SNR (signal to noise ratio) than ^{19}F MAS NMR spectra although each sample was run for at least 48 h. ^{13}C MAS NMR via cross-polarization by fluorine would help to reduce the relaxation time considerably. However cross-polarization data are not accurately quantifiable as the resonances are excited unequally. This is especially the case as the structural fluorine is reduced by lithiation. Two clear peaks were prominent despite the low SNR. The one around 82 to 90 ppm is assigned to CF[5] as shown in Fig. 10. The graphitic carbon is present around 125 ppm[6] while CF_2 and Teflon^{TM} peaks are overlapped heavily with the broad graphite carbon peak. As in the case of the ^{19}F results, the intensity of the Teflon^{TM} peak is not included in the ^{13}C deconvolutions which are displayed in Fig. 11.

In the ^{13}C MAS NMR spectra the CF peak resonates at 84–88 ppm. The ^{13}C NMR chemical shift of a carbon in a semi-ionic/ionic interaction with fluorine is near 89 ppm. Therefore this peak is not distinguishable from the covalent resonance. There are three closely spaced main features around −125 to −108 ppm assigned to bulk graphite, Teflon^{TM} and components that are generally attributed to CF_2 groups on the edge of the graphite planes. However, unlike the CF_2 edge groups seen in the ^{19}F MAS NMR data, this resonance disappears upon complete discharge. A complication, however, is the overlap of the broad graphite resonance, which of course becomes a severe problem for deconvolution at successively higher DoD. It is therefore concluded that if this is indeed representative of CF_2 groups, they are bound differently to the bulk CF, and are more accessible (e.g. surface vs. bulk sites) to the lithium than those seen in the fluorine data. However it is noted that even the ^{19}F data show decreasing CF_2 content with increasing DoD.

An sp^3 bonded carbon species around 55 ppm and another around 65 ppm, also assigned to sp^3 bonded carbon, appears in the middle stage of the electrochemically discharge samples. The

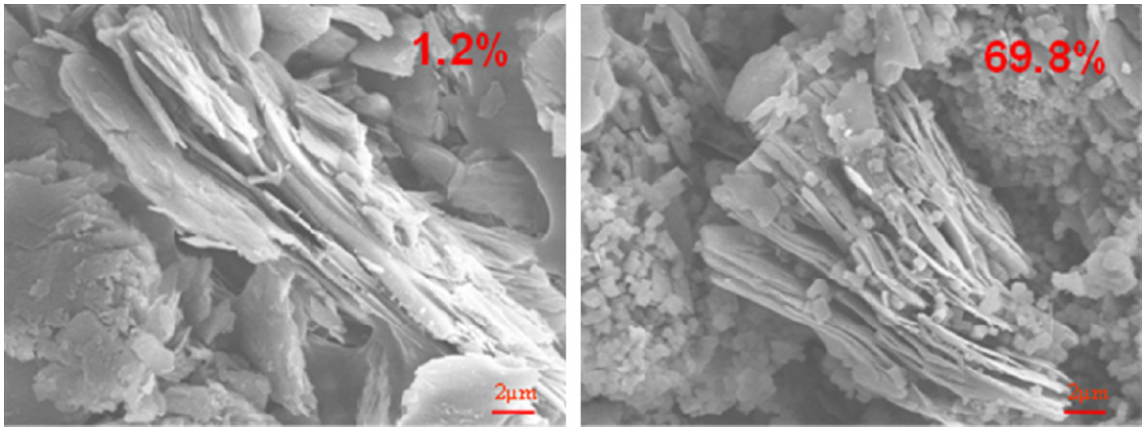

Fig. 6. SEM image of CF_x C at 1.2% DoD and CF_x C at 69.8% DoD.

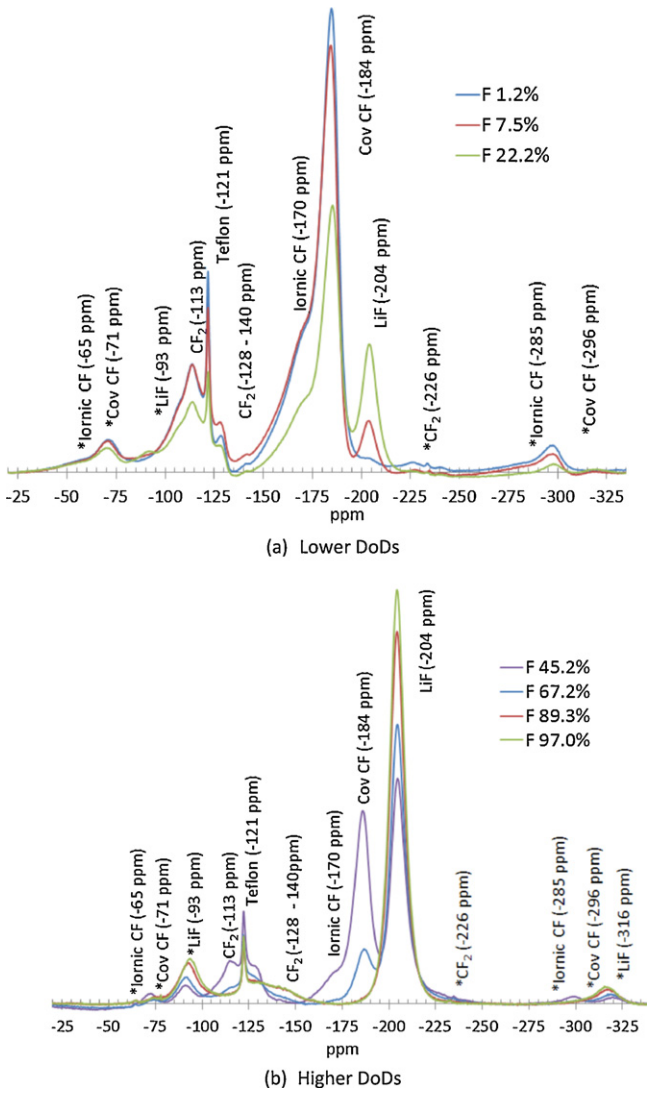

Fig. 8. ^{19}F MAS NMR spectra of Greatbatch discharged F Series. Asterisks denote spinning sidebands.

F series shows the maximum sp^3 bonded carbon amount which increases steadily from the middle to the end of discharge. The increase in bulk graphite content with increased discharge is also a consistent trend. Overall, the C series has the lowest CF consumption for a given nominal DoD while F and G maintain comparable amounts.

In order to check for possible differences in LiF formation between CF_x types, spin–lattice relaxation (T_1) measurements were performed. LiF is the only compound that appears in the ^{7}Li spectra as shown in Fig. 12. There is a clear increase of T_1 in all the series with increasing DoD. ^{7}Li T_1 of C and G series increase more slowly in comparison to the F series as shown in Fig. 13. One possible interpretation is that LiF precipitates out of the C/CF_x structure of the F series more readily as it more rapidly approaches bulk-like characteristics (i.e. longer T_1). Similar behavior of increasing T_1 with increasing DoD was observed in the ^{19}F measurements as shown in Fig. 14. Finely dispersed nanoscopic LiF that is formed in the early stages of discharge is generally characterized by shorter T_1 values compared to its bulk macroscopic phase due to structural defects. The more rapid exclusion of LiF may be an explanation of the superior performance of the F series material, since LiF is an insulator. For completeness, a ^{7}Li NMR spectrum of a nearly completely discharged sample is displayed in Fig. 12, and the spectrum is identical

Fig. 9. ^{19}F MAS NMR deconvolution of Greatbatch discharged F, C and G series.

in appearance to that of bulk LiF. Debye-Scherrer analysis of LiF XRD peak widths showed an increase of crystallite size from low DoD values (<10%) which appeared to level off by 40% DoD. There was no conclusive difference observed between the different forms of CF_x, indicating that in the LiF product formed from these lithiated CF_x samples, NMR, as a short-range structural probe, is more sensitive to lattice strains and defects than XRD.

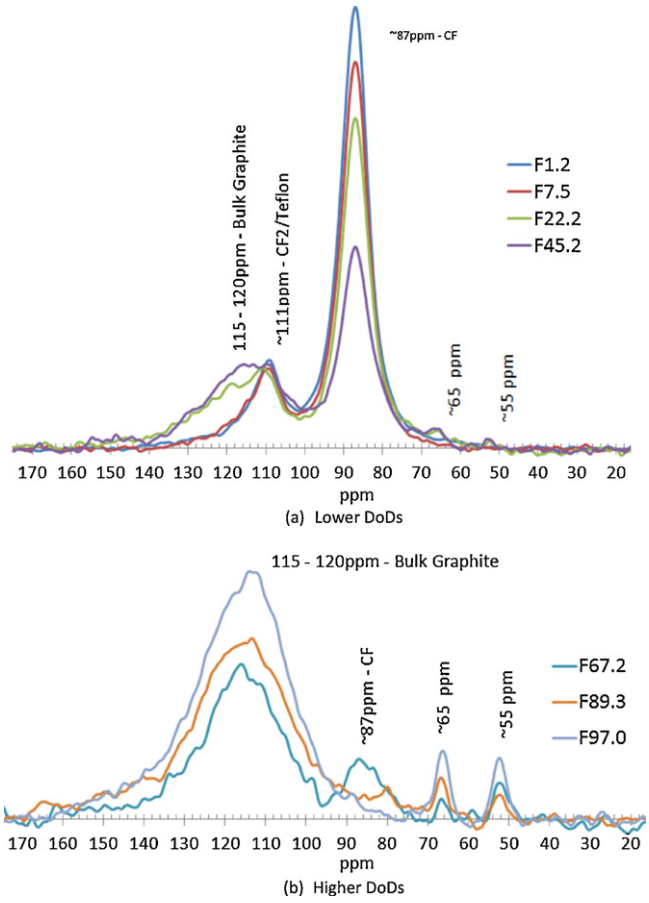

Fig. 10. ^{13}C MAS NMR spectra of Greatbatch discharged F series.

3.3. Hunter discharged batteries

All the samples were run under comparable conditions described for the previous set. Although washed samples were rinsed with DME, a significant amount of $LiAsF_6$ was present in the samples as indicated by the feature at −69.5 ppm overlapped with left sidebands of LiF (slightly overlapped) and covalent CF (heavily overlapped) as shown in Fig. 15. Some samples were run at slightly lower spinning speed (32 kHz) due to mechanical issues and hence slight differences in the positions of sidebands are observed in the spectra. One clear observation is the LiF contents of Hunter discharged batteries are higher than those of Greatbatch discharged batteries especially in F and G series. That is, the actual LiF content is higher than the amount prescribed by the nominal DoD value. The reason for this could be the inhomogeneity of the sample in the different parts of the cathode which experienced different discharge rates. The ^{19}F deconvolutions are displayed in Fig. 16. It appears that all of the semi-ionic CF is consumed at the higher DoDs which is consistent with the results for the slower discharged samples.

^{13}C MAS NMR spectra reveal more subtle but important details. Three representative sets of spectra are displayed in Figs. 17–19, for washed and unwashed samples. The unwashed samples are characterized by large residual solvent peaks, despite the post-rinse vacuum treatment. The spectral intensity ratios of the two main peaks, graphite and CF, are similar in the washed and unwashed samples. Only F series consistently shows both features assigned to sp^3 bonded carbon at 55 and 65–68 ppm as in Greatbatch slow discharged samples. C series shows two sp^3 bonded carbon peaks in the same region. However at 80% DoD the peak around 65–68 ppm

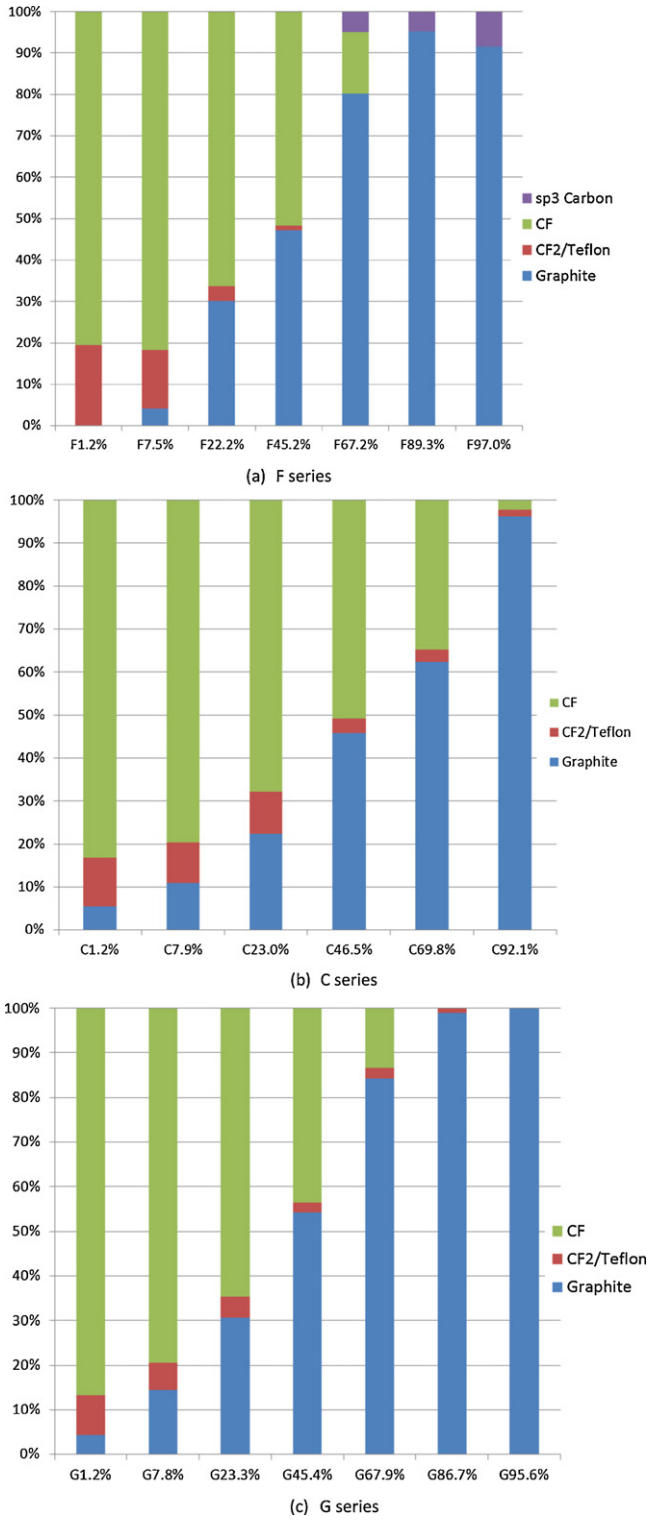

Fig. 11. ^{13}C MAS NMR deconvolution of Greatbatch discharged F, C and G Series. The spectral results of C at 99.4% DoD are not included due to the low SNR characteristics of that sample. Although CF intensity appears in the ^{19}F spectra for the ~89% DoD samples, it does not show up distinctly in the ^{13}C deconvolutions due to large overlap.

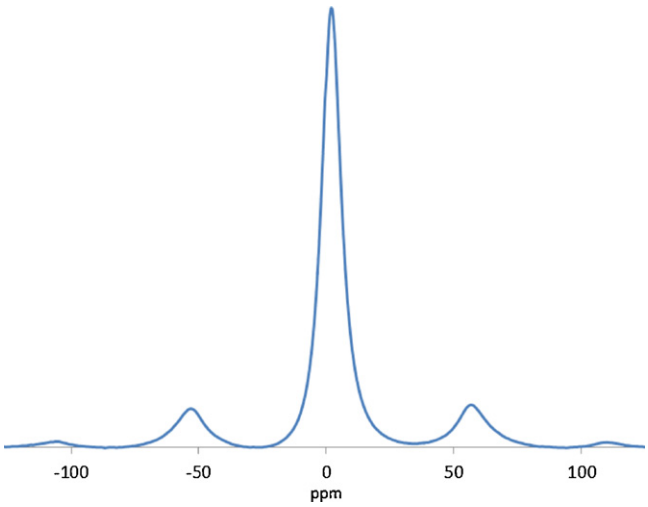

Fig. 12. ^{7}Li MAS NMR spectrum of Greatbatch 99.4% discharged F sample.

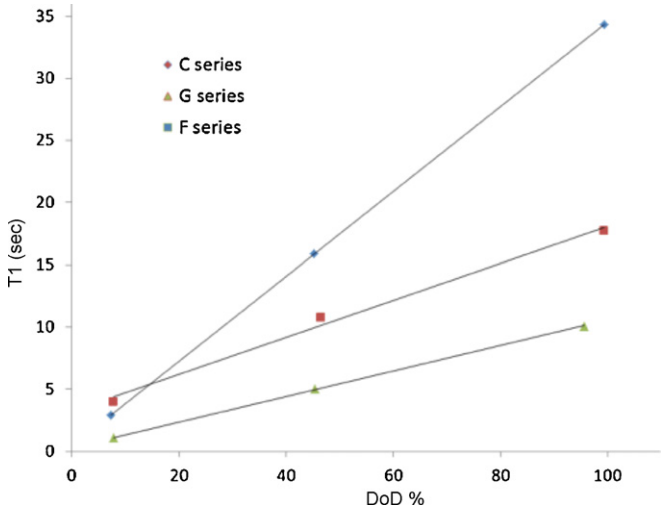

Fig. 13. ^{7}Li MAS NMR T_1 measurements of Greatbatch discharged batteries. The straight lines are guides to the eye.

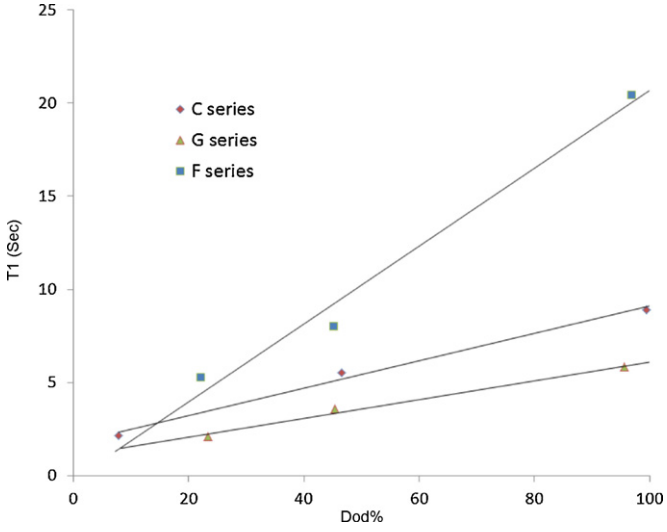

Fig. 14. ^{19}F MAS NMR T_1 measurements of Greatbatch discharged batteries. The straight lines are guides to the eye.

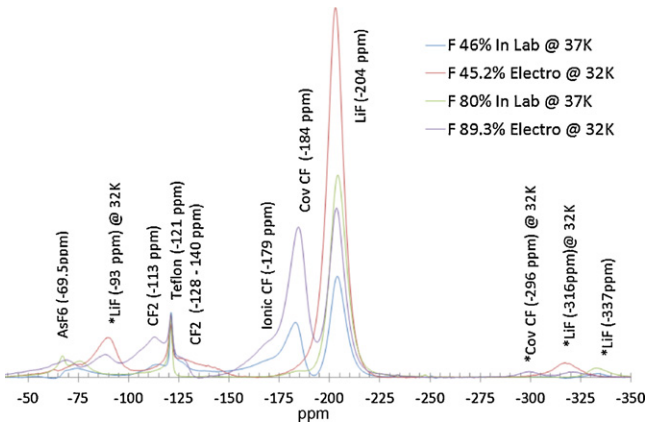

Fig. 15. ^{19}F MAS NMR spectra of Hunter and Greatbatch discharged batteries. Asterisks denote spinning sidebands.

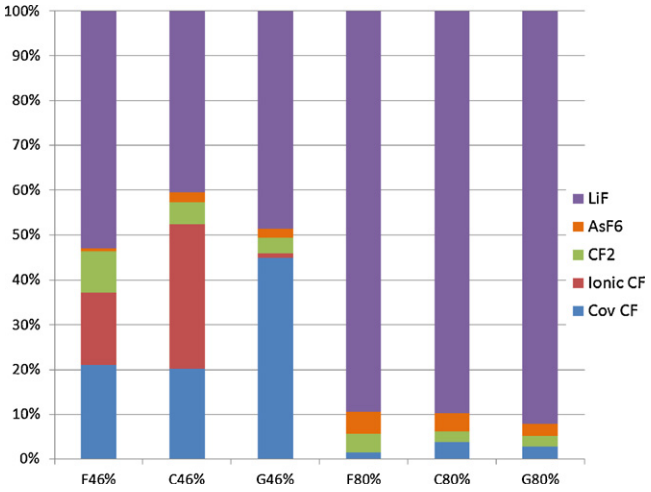

Fig. 16. MAS NMR spectra of Hunter discharged batteries for F, C and G series.

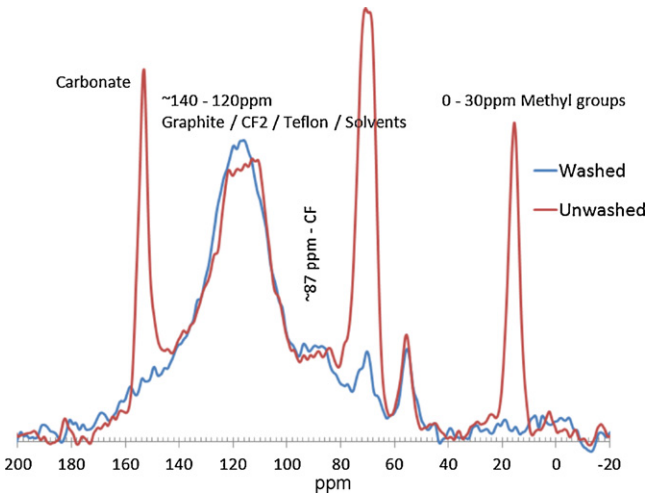

Fig. 17. MAS NMR spectra of Hunter 80% discharged F series.

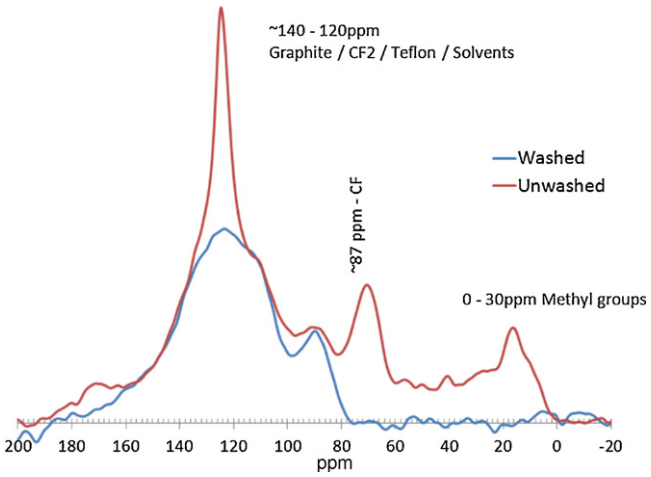

Fig. 18. ^{13}C MAS NMR spectra of Hunter 46% discharged G series.

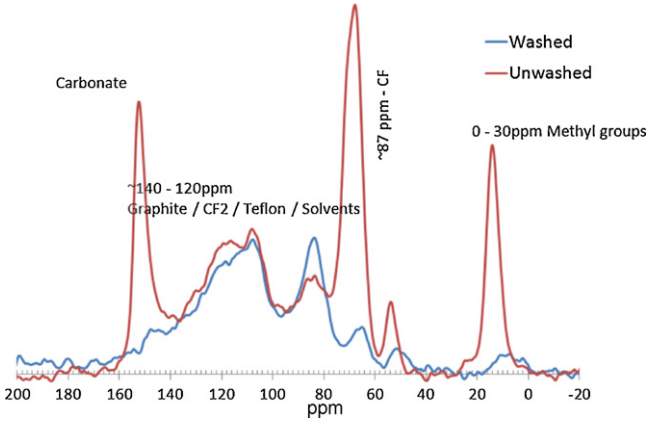

Fig. 19. ^{13}C MAS NMR spectra of Hunter 46% discharged C series.

was absent. Also the peak around 55 ppm is not as strong as it is in the 46% DoD sample. The G Series is quite different. At 46%, no peaks are observed around 55 and 65–68 ppm. However a small peak around 65 ppm is observed at 80% DoD.

4. Conclusions

^{19}F and ^{13}C NMR of electrochemically lithiated CF_x of different morphologies reveal largely similar behavior of LiF formation. Unlike chemically lithiated samples [2] the semi-ionic CF consumption is faster than covalent CF in electrochemically discharged cells. Samples undergoing relatively fast discharge exhibit higher LiF contents at the corresponding DoD values, most likely due to inhomogeneity. An important observation was that no metastable compounds detectable by ^{19}F or ^{13}C NMR were found in the fast discharged samples. ^{13}C MAS NMR data also showed some similar behavior of carbon formation. For all three types of CF_x. However one significant observation was the consistent appearance of sp^3 bonded carbon in the F series at higher DoD values. Given the superior performance of the F series at higher DoD values, it is surmised that there is a structural rearrangement of the carbon lattice involving sp^3 bonded carbon which stabilizes the material at high DoD levels. Supporting evidence for the stability of F-type CF_x comes from both ^{7}Li and ^{19}F T_1 measurements which suggest that LiF formed upon discharge is excluded from the structure of the material more readily than in the C and G series.

Acknowledgements

Hunter College acknowledges an infrastructure grant from the National Institutes of Health (RR 003037), as well as an instrumentation grant from the office of Naval Research. The authors are grateful for the financial support provided by the Center for Advanced Technology in Photonics Applications at The City University of New York, designated by the New York State Foundation for Science, Technology and Innovation (NYSTAR).

References

[1] T.B. Reddy, Handbook of Batteries, 4th ed., McGraw-Hill, New York, 2010 (Chapter 14).
[2] N.D. Leifer, V.S. Johnson, R. Ben-Ari, H. Gan, J.M. Lehnes, R. Guo, W. Lu, B.C. Muffiletto, T. Reddy, P.E. Stallworth, S.G. Greenbaum, J. Electrochem. Soc. 157 (2010) A148–A154.
[3] R. Thomas, Krawietz, F. James, Chem. Commun. (1998) 2151–2152.
[4] Jerome Giraudet, Marc Dubois, Katia Guerin, Andre Hamwi, Francis Masin, J. Phys. Chem. Sol. 67 (2006) 1100–1105.
[5] J. Giraudet, M. Dubois, K. Guerin, C. Delabarre, P. Pirotte, A. Hamwi, F. Masin, Sol. State NMR 31 (2007) 131–140.
[6] M. Dubois, K. Guerin, J.P. Pinherio, Z. Fawal, F. Masin, A. Hamwi, Carbon 42 (2004) 1931–1940.